

# Large-scale statistical forecasting models reassess the unpredictability of chaotic systems

William Gilpin\*

*Department of Physics, The University of Texas at Austin, Austin, Texas 78712, USA and  
Oden Institute for Computational Engineering and Sciences,  
The University of Texas at Austin, Austin, Texas 78712, USA*

(Dated: April 28, 2023)

Chaos and unpredictability are often considered synonymous, yet recent advances in statistical forecasting suggest that large machine learning models gain unexpected insight from extended observation of complex systems. We perform a large-scale comparison of 24 state-of-the-art multivariate forecasting methods on a crowdsourced database of 135 distinct low-dimensional chaotic systems. Large, domain-agnostic time series forecasting methods consistently exhibit the strongest performance, producing accurate predictions lasting up to two dozen Lyapunov times. The best-performing models contain no inductive biases for dynamical systems, and include hierarchical neural basis functions, transformers, and recurrent neural networks. However, physics-based hybrid methods like neural ordinary differential equations and reservoir computers perform more strongly in data-limited settings. Diverse forecasting methods correlate despite their widely-varying architectures, yet the Lyapunov exponent fails to fully explain variation in the predictability of different chaotic systems over long time horizons. Our results show that a key advantage of modern forecasting methods stems not from their architectural details, but rather from their capacity to learn the large-scale structure of chaotic attractors.

## I. INTRODUCTION

Chaos traditionally implies the butterfly effect: a small change in a system grows exponentially over time, complicating efforts to reliably forecast the system's long-term evolution. Predicting chaos has therefore represented a longstanding problem at the interface of physics and computer science [1], motivating some of the earliest applications of artificial neural networks during the 1991 Santa Fe forecasting competition [2].

Recent successes in statistical forecasting motivate revisiting this problem, by providing compelling examples of data-driven prediction of diverse systems such as cellular signaling pathways [3], hourly precipitation forecasts [4], active nematics [5], and tokamak plasma disruptions [6]. These advances complement recent theoretical works showing that large, overparameterized statistical learning methods learn latent representations of complex systems that implicitly linearize dynamics, raising the possibility of forecasting even strongly-chaotic systems using models with sufficient capacity [7–9]. Such results potentially explain the emergence of reservoir computers as best-in-class forecasting methods for dynamical systems [10–16]; these models use emergent properties of random networks to lift complex time series into a random feature space, thereby simplifying learning at the expense of increasing model complexity [17, 18]. Other recently-introduced hybrid models directly encode dynamical constraints within their model formulation [19]; among these are neural ordinary differential equations [20], physics-informed neural networks [21], and recurrent neural networks with domain-specific architectures [22–24].

However, there is little consensus whether the practical success of emerging forecasting methods stems from fundamental advances in representing and parameterizing chaos, or simply from the availability of larger datasets, model capacities, and computational resources [25–27]. Moreover, a lack of systematic comparison among methods ambiguates the process of selecting a forecasting method for a given dynamical system—especially the question of whether dynamical constraints should be encoded into a model or learned from large datasets in a domain-agnostic manner. The former provides an inductive bias that economizes training, while the latter allows greater flexibility and reduces model selection bias. Complicating comparisons among methods are the widely-varying contexts in which prior methods have been evaluated, which range from domain-specific weather or biomedical time series to well-known individual chaotic systems like the Lorenz attractor [24, 27–30]. A larger set of representative systems, and a controlled comparison among methods, is necessary to disentangle the relationship between chaoticity, predictability, and forecasting model architecture, as well as to understand how the properties of different black-box machine learning methods interact with the systems they predict.

Here, we systematically quantify the relationship between chaos and empirical predictability in a large-scale, controlled experiment. We created a benchmark dataset containing 135 low-dimensional differential equations describing known chaotic attractors [31]. Originally curated from published works to include well-known systems such as the Lorenz, Rössler, and Chua attractors, the dataset has grown through crowdsourcing to include examples spanning diverse domains such as climatology, neuroscience, and astrophysics. Each dynamical system is aligned with respect to its dominant timescale and inte-

\* [wgilpin@utexas.edu](mailto:wgilpin@utexas.edu)

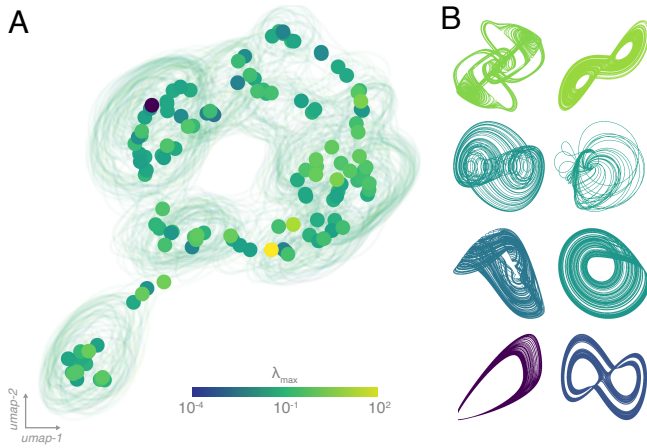


**Figure 1. A space of chaotic dynamical systems.** (A) A nonlinear embedding of 135 distinct low-dimensional chaotic systems, colored by largest Lyapunov exponent ( $\lambda_{\max}$ ). Contours denote 50% confidence intervals in the embedding of each system over 500 random initial conditions and feature subsets; points denote centroids for each system. (B) Example systems from the dataset, colored by  $\lambda_{\max}$ .

gration timestep using surrogate significance testing [32], and is annotated with calculations of its invariant properties such as the Lyapunov exponent spectrum, fractal dimension, and metric entropy.

Although each system has a different largest Lyapunov exponent ( $\lambda_{\max}$ )—which indicates its putative chaoticity—some systems are more closely related to each other than to others. For example, the 19 members of the Sprott attractor subfamily ( $\lambda_{\max} \in [0.01, 1.1]$ ) exhibit similar qualitative structure such as paired lobes, owing to the presence of predominantly quadratic nonlinearities in the governing differential equations [33, 34]. To identify such relationships across our dataset, we convert each dynamical system into a high-dimensional vector by first generating a long trajectory, and then computing 747 characteristic mathematical signal properties such as the metric entropy, power spectral coefficients, Hurst exponents, and others that are invariant to the initial conditions and sampling rate [35, 36]. We then use uniform manifold approximation and projection (UMAP) to visualize these high-dimensional vectors in a two-dimensional plane (Fig. 1) [37, 38]. The resulting space of chaotic systems shows clear structure, with the Sprott and other scroll-like subfamilies clustering together, while qualitatively distinct systems separate. These results suggest that our dataset contains high dynamical diversity beyond absolute chaoticity  $\lambda_{\max}$ , which correlates only weakly with the embedding ( $\rho = 0.15 \pm 0.03$ , bootstrapped Spearman rank-order coefficient).

Our dataset allows us systematically compare the forecasting ability of different statistical forecasting methods across diverse dynamical systems. Forecasting dynamical systems from observations is a well-established field [32], and we structure our experiments as a standard long-

term autoregressive forecasting task [39]. For each dynamical system, we define two time series  $Y_{\text{train}}, Y_{\text{test}} \in \mathbb{R}^{T \times D}$  corresponding to multivariate trajectories emanating from different initial conditions, and we define a splitting time such that  $T = T_{\text{past}} + T_{\text{fut}}$ ,  $Y_{\text{train}} = Y_{\text{train}}^{\text{past}} \cup Y_{\text{train}}^{\text{fut}}$ , etc. The model parameters are first fit using  $Y_{\text{train}}^{\text{past}}$ , and the accuracy of the resulting predictions on  $Y_{\text{train}}^{\text{fut}}$  are used for model selection and hyperparameter tuning. After completing model selection, the final model from each model class is then fit on  $Y_{\text{test}}^{\text{past}}$ , and the resulting predictions on the heretofore-unseen  $Y_{\text{test}}^{\text{fut}}$  produce the error score  $\epsilon_{ik}(t)$  representing the performance of the  $i^{\text{th}}$  forecasting model on the  $k^{\text{th}}$  dynamical system at a horizon  $t \in [0, T_{\text{fut}}]$  after the end of training data availability. We compute 17 different error metrics, including root mean-squared error, pointwise correlation, mutual information, and Granger causality. We report our results in the main text in terms of the symmetric mean absolute percent error (sMAPE)  $\epsilon(t) \equiv (2/t) \sum_{t'=1}^t (|\mathbf{y}(t') - \hat{\mathbf{y}}(t')|) / (|\mathbf{y}(t')| + |\hat{\mathbf{y}}(t')|)$  due to its common use, conceptual simplicity, and correlation with other metrics [8, 27, 28, 31, 40].

Each forecasting method represents a class of possible models parameterized by choices made regarding architecture (model size, number of layers, activation function) or training (optimization epochs, batch sizes). Such choices can strongly affect the performance of different methods [12, 27, 32], yet different methods do not necessarily have equivalent adjustable hyperparameters. In order to fairly compare different methods, we restrict hyperparameter tuning to the equivalent of the input time window for each model—such as the input size for deep neural networks, order of autoregressive models, leakage rate for reservoir computers, or time lags for state space models. We tune hyperparameters separately on each system and forecasting model pair. Our overall experiment design is characterized by several timescales: the *lookback window* hyperparameter corresponds to the number of past timepoints seen simultaneously by a model at a given time during training and prediction; the *history length* represents the total number of timepoints available to learn the model’s parameters before prediction; the *forecast horizon* represents the number of unseen timepoints into the future that are predicted autoregressively; and the *Lyapunov time*  $\lambda_{\max}^{-1}$  is an invariant property of each distinct dynamical system, representing the characteristic timescale over which forecasts are expected to lose accuracy due to the butterfly effect.

We evaluate 24 statistical forecasting models across all 135 dynamical systems. We choose forecasting methods representative of the broad diversity of methods available in the recent literature [25, 41]. Traditional methods include standard linear regression, autoregressive moving averages (ARIMA), exponential smoothing, Kalman filtering, Fourier mode extrapolation, boosted random forest models [32], and newly-introduced linear models that account for trends and distribution shift [42]. Current state-of-the-art models for general

time series forecasting are based on deep neural networks: the transformer model [43], long-short-term-memory networks (LSTM), vanilla recurrent neural networks (RNN), temporal convolutional neural networks [30], and neural basis expansion/neural hierarchical interpolation (NBEATS/NHiTS) [44, 45]. The latter methods generate forecasts hierarchically by aggregating separate forecasts at distinct timescales (NBEATS), and can explicitly coarse-grain the time series to further reduce computational costs (NHiTS). We also consider hybrid physics-motivated methods such as neural ordinary differential equations [20], which approximate the continuous-time differential equation underlying time series, as well as echo-state networks and their generalization, nonlinear vector autoregressive models (nVAR), which train a linear model on a fixed “reservoir” of random nonlinearities [10, 17, 18].

Our long-term forecasting experiments require  $\sim 10^{19}$  floating point operations for training, model selection, and hyperparameter tuning, a figure comparable to the scale of other recent large-scale machine learning benchmarks [46]. For brevity, we highlight results for the best-performing forecasting models, and defer the full tabular results and alternative accuracy metrics to the supplementary material and our open-source repository.

Our main results are summarized in Figure 2. We observe that modern learning statistical methods successfully forecast diverse chaotic systems, with the strongest methods consistently succeeding across diverse systems and forecasting horizons. We highlight the strong relative performance of machine learning models in Fig 2C, where NBEATS successfully forecasts the Mackey-Glass equation for  $\sim 22$  Lyapunov times without losing track of the global phase (see Fig. S1 for additional examples). Across all systems, the best-performing models achieve an average valid prediction time equal to  $14 \pm 2 \lambda_{\max}^{-1}$ . These results extend beyond the  $\sim 10 \lambda_{\max}^{-1}$  reported in recent works [13, 39], and sharply improves on the  $\sim 5 \lambda_{\max}^{-1}$  typically achieved before the widespread adoption of large machine learning models [32]. Our results underscore rapid progress since the  $\sim 1 \lambda_{\max}^{-1}$  targeted in the original Santa Fe competition [2]. The strongest-performing methods include NBEATS, transformers, and LSTM, which are all large models originally designed for generic sequential datasets, and which do not assume that input time series arise from a dynamical system. This observation suggests that more flexible, generic architectures may prove preferable for problems where some physical structure is present (e.g., analytic generating functions in the form of ordinary differential equations) but stronger domain knowledge (e.g., symmetries or symplecticity) is unavailable to further constrain learning.

The strong performance of NBEATS/NHiTS suggests that this model has structural features favoring the chaotic systems dataset. Prior work has shown that hierarchical forecasting methods can flexibly integrate information across multiple timescales in a manner inaccessible to classical statistical models [45]. While chaotic sys-

tems exhibit continuous spectra and thus contain information relevant to forecasting at a variety of timescales, many systems exhibit topologically-preferred timescales such as unstable periodic orbits—like the “loops” on either side of the Lorenz attractor—that dominate the system’s underlying measure [47], and which therefore may represent higher priority motifs for learning. Highly performant model architectures therefore likely contain implicit inductive biases that advantage them on chaotic systems relative to other time series. Consistent with this finding, we note that reservoir computers (nVAR/Echo State Networks) also perform strongly on the chaotic systems dataset [17, 18], consistent with prior observations for individual chaotic systems [10–16].

While the utility of deep learning methods for forecasting general time series has been questioned [27, 28], our results agree with recent benchmarks suggesting that large models strongly outperform classical forecasting methods on long-horizon forecasting tasks [43]. We find that classical methods like exponential smoothing or ARIMA do not appear among the top models, implying that the size and diversity of our chaotic systems dataset, as well as the long duration of the forecasting task, require larger models with greater intrinsic capacity to represent complex nonlinear systems. Relative performance among models remains stable across two orders of magnitude in Lyapunov time, indicating that strong models better approximate the underlying propagator for the flow even at small forecasting horizons. Given the autoregressive nature of forecasting, an initial accuracy advantage compounds over time due to the exponential sensitivity of chaotic systems to early errors. However, in the supplementary material we show that the best-performing models *also* reproduce dynamical invariants such as Lyapunov exponent spectra and fractal dimensions better than other methods, suggesting that pointwise forecast accuracy is a prerequisite to accurately reconstructing dynamical manifolds.

While domain-agnostic time series methods perform well, we note that the different forecasting methods have different intrinsic model complexities and thus capacities. Fig. 3A shows the forecasting error at  $\lambda_{\max}^{-1}$  versus the computational walltime required to train each model on one central processing unit. Training walltime measures model efficiency, and we interpret it as a loose proxy for model complexity because model size and trainable parameter count are not directly quantifiable across highly-distinct and regularized architectures [46]. We find that error and training time exhibit negative correlation ( $\rho = -0.31 \pm 0.04$ , bootstrapped Spearman coefficient), which persists within most method groups. The best-performing machine learning models require considerable training times; in contrast, reservoir computers exhibit competitive performance with two orders of magnitude less training time due to their linear structure. The strong performance of reservoir computers implicates an inductive bias for learning complex dynamical systems, due to their disordered reservoir allowing them to more

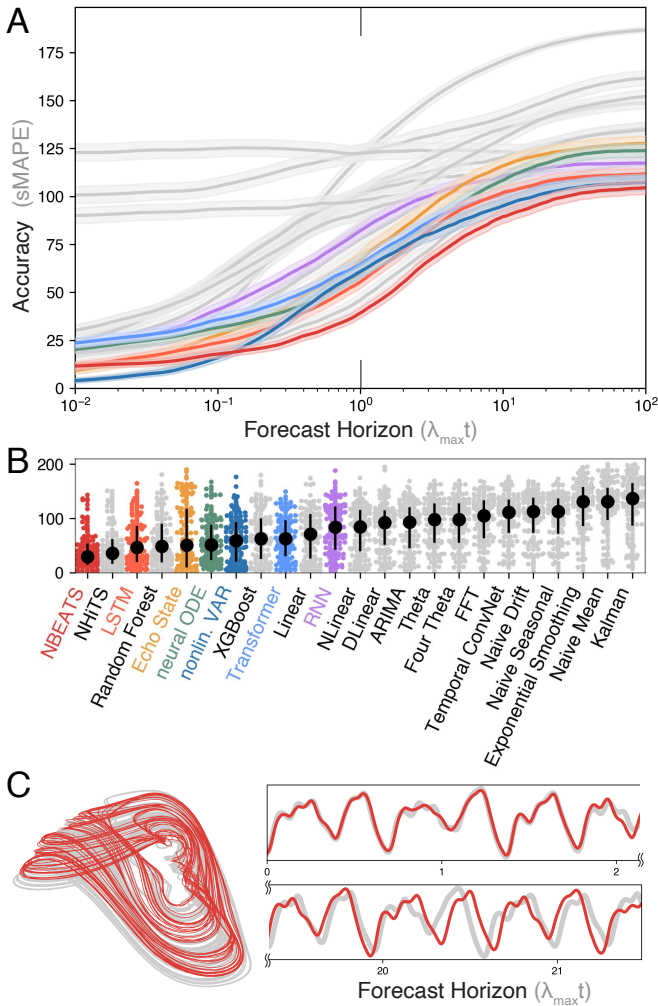


**Figure 2. Statistical forecasting across an ensemble of chaotic systems.** (A) The average error of all 24 forecasting methods  $\langle \epsilon_{ik}(t) \rangle_k$  as a function of Lyapunov time, averaged across 135 distinct chaotic systems. Colors denote high-performing models with properties of particular interest. (B) Distributions of the forecast errors when  $t = \lambda_{\max}^{-1}$ . (C) The predictions of the best-performing forecast model (red), relative to a held-out true trajectory from the Mackey-Glass model (gray) at short and long forecasting horizons.

readily represent continuous spectra [18, 48–50]. Conversely, the transformer model has high intrinsic capacity and low inductive bias for dynamical systems [43], and thus requires the most computational resources.

This general tradeoff between performance and training difficulty motivates us to search for universal similarities across different forecasting methods. In Fig. 3B we compute the time-resolved Spearman correlation between each method’s forecast error and the average error of that method,  $\tilde{\rho}_i(t) = \rho(\epsilon_{ik}(t), \langle \epsilon_{ik} \rangle_t)_k$ . We find universal non-monotonic behavior, in which nearly all methods exhibit peak correlation at one Lyapunov time  $\lambda_{\max}^{-1}$  (Fig. 3B). This observation underscores that the largest Lyapunov exponent represents an appropriate timescale for comparing different dynamical systems, and that diverse forecasting models interact with this property in a shared manner.  $\lambda_{\max}^{-1}$  is sufficiently long to distinguish dynamical systems based on their invariant properties, but short enough that forecast methods do not accrue instabilities, large phase offsets, and other artifacts that saturate forecast error and mask intrinsic differences among systems. This observation aligns with recent work on statistical learning theory that draws analogies between trained learning models and disordered systems [51]: when models become most strongly coupled to the specific properties of individual systems, they exhibit peak correlation with their mean-field prediction. Additionally, we find the predictions of different large models become correlated at long forecasting horizons, suggesting that they agree on which particular dynamical systems prove hardest to forecast (see Fig. S4). Surprisingly, their performance only weakly correlates with  $\lambda_{\max}^{-1}$  and thus intrinsic chaoticity, with any correlation vanishing at long forecasting horizons.

Taken together, these results suggest that the greater intrinsic capacity and flexibility of overparameterized domain-agnostic models allows them to access a new long-horizon forecasting regime, in which their forecast accuracy decorrelates with Lyapunov exponent—and thus intrinsic chaoticity. To further investigate model complexity and performance, we next perform a series of experiments in which we titrate the history length, which determines the total amount of training data available to each method before generating a forecast (Fig. 3C). Unlike training time or parameter count, this quantity determines how effectively different methods utilize additional observations. As expected, all models asymptotically improve given more training data. However, the best-performing models improve more quickly and reach lower asymptotes as the available history increases, suggesting that they better leverage additional data than less performant models. These results match the intuition that these models combine high intrinsic capacity with inductive biases for chaotic dynamical systems in order to outperform other methods on our dataset.

Our results show that recently-developed large, overparameterized statistical forecasting models efficiently leverage long-term observations of chaotic attractors, producing best-in-class forecasts that can remain accurate for up to two dozen Lyapunov times. Commonalities in predictions across highly distinct model classes suggest that performance arises primarily from model capacity and generalization ability, rather than specific architectural choices, and that performance at long prediction times is ultimately limited by a model’s ability to learn long-term properties of a dynamical system’s underlying attractor—rather than just local geometry encoded by the Lyapunov exponent. The strong performance of generic large models echoes recent findings from other domains and represent an intuitive consequence of

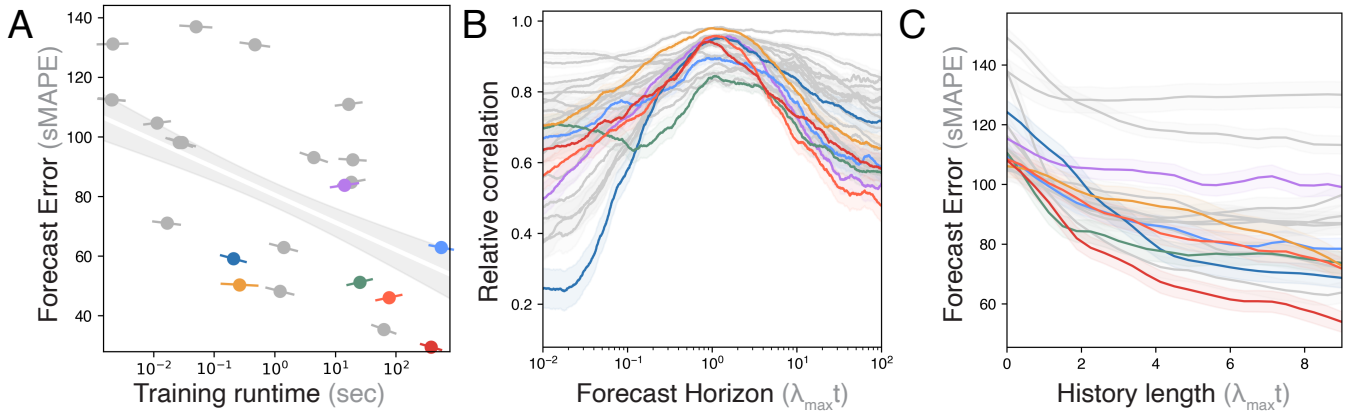


**Figure 3. Universal relationships among forecasting methods.** (A) Error versus training time at fixed forecast horizon  $t = \lambda_{\max}^{-1}$  for all models. Bar lengths denote standard deviations along principle axes, with angle indicating Spearman correlation within each model group in order to check for Simpson’s paradox. The underlaid linear fit indicates the overall correlation  $\rho = -0.31 \pm 0.04$ . (B) Median relative correlation of each forecasting method with its average prediction, across different forecast horizons. (C) Median model errors at  $t = \lambda_{\max}^{-1}$  as the amount of history data increases. All error bars correspond to 95% confidence intervals, and colors match methods from previous figures.

the “no free lunch” theorem for model selection [52, 53]. Nonetheless, our results are practically informative for forecasting real-world time series driven by underlying dynamical systems. In the absence of restrictions on data availability or training resources, large domain-agnostic models are likely to produce high-quality forecasts without the need for system-specific knowledge. However, in restricted settings, domain-specific methods such as reservoir computers exhibit the strongest performance relative to their computational requirements [10].

While certain methods perform particularly well in our experiments, we refrain from endorsing specific models to the detriment of others: our results may be specific to our chaotic systems dataset and, more importantly, the recent literature contains a broad variety of new forecasting models, as well as infinite possible variations of each method due to hyperparameter and architectural choices, which could potentially exhibit comparable performance. Rather, we have chosen representative set of forecasting models bridging different foci of the literature [25, 28], and highlight general trends and the emerging strength of new models on the classical problem of forecasting chaos.

Our observation that  $\lambda_{\max}$  fails to fully determine whether a system remains empirically predictable over extended horizons suggests the need, in future work, to relate our empirical forecasting results to invariant prop-

erties of the different dynamical systems in our dataset, such as various measures of fractality and entropy [26]. Such characterization could improve the interpretability of machine learning-based forecasting models, which ostensibly provide less insight into a time series’s structure than classical methods [27, 44]. However, the strong empirical performance of machine learning suggests the potential for these methods to reveal new properties of nonlinear dynamics and, ultimately, new bounds on the intrinsic predictability and thus reducibility of chaotic systems.

## II. ACKNOWLEDGMENTS

We thank Harry Swinney and Phil Morrison for informative discussions. W. G. was supported by the University of Texas at Austin. Computational resources for this study were provided by the Texas Advanced Computing Center (TACC) at The University of Texas at Austin.

## III. CODE AVAILABILITY

All code used in this study is available online at <https://github.com/williamgilpin/dysts>

---

[1] Boffetta, G., Cencini, M., Falcioni, M. & Vulpiani, A. Predictability: a way to characterize complexity. *Physics reports* **356**, 367–474 (2002).

[2] Weigend, A. S. & Gershenfeld, N. A. Results of the time series prediction competition at the santa fe institute. In *IEEE International Conference on Neural Networks*, 1786–1793 (IEEE, 1993).

[3] Yazdani, A., Lu, L., Raissi, M. & Karniadakis, G. E. Systems biology informed deep learning for inferring parameters and hidden dynamics. *PLoS Computational Biology* **16**, e1007575 (2020).

[4] Espeholt, L. *et al.* Deep learning for twelve hour precipitation forecasts. *Nature Communications* **13**, 5145 (2022).

[5] Colen, J. *et al.* Machine learning active-nematic hydrodynamics. *Proceedings of the National Academy of Sciences* **118**, e2016708118 (2021).

[6] Zheng, W. *et al.* Hybrid neural network for density limit disruption prediction and avoidance on j-text tokamak. *Nuclear Fusion* **58**, 056016 (2018).

[7] Brunton, S. L., Brunton, B. W., Proctor, J. L., Kaiser, E. & Kutz, J. N. Chaos as an intermittently forced linear system. *Nature communications* **8**, 19 (2017).

[8] Wang, R., Dong, Y., Arik, S. O. & Yu, R. Koopman neural forecaster for time series with temporal distribution shifts. In *International Conference on Machine Learning* (PMLR, 2023).

[9] Otto, S. E. & Rowley, C. W. Koopman operators for estimation and control of dynamical systems. *Annual Review of Control, Robotics, and Autonomous Systems* **4**, 59–87 (2021).

[10] Gauthier, D. J., Bollt, E., Griffith, A. & Barbosa, W. A. Next generation reservoir computing. *Nature communications* **12**, 5564 (2021).

[11] Bompas, S., Georgeot, B. & Guéry-Odelin, D. Accuracy of neural networks for the simulation of chaotic dynamics: Precision of training data vs precision of the algorithm. *Chaos: An Interdisciplinary Journal of Nonlinear Science* **30**, 113118 (2020).

[12] Platt, J. A., Wong, A., Clark, R., Penny, S. G. & Abarbanel, H. D. Robust forecasting using predictive generalized synchronization in reservoir computing. *Chaos: An Interdisciplinary Journal of Nonlinear Science* **31**, 123118 (2021).

[13] Pathak, J., Hunt, B., Girvan, M., Lu, Z. & Ott, E. Model-free prediction of large spatiotemporally chaotic systems from data: A reservoir computing approach. *Physical review letters* **120**, 024102 (2018).

[14] Jiang, J. & Lai, Y.-C. Model-free prediction of spatiotemporal dynamical systems with recurrent neural networks: Role of network spectral radius. *Physical Review Research* **1**, 033056 (2019).

[15] Chattopadhyay, A., Subel, A. & Hassanzadeh, P. Data-driven super-parameterization using deep learning: Experimentation with multiscale lorenz 96 systems and transfer learning. *Journal of Advances in Modeling Earth Systems* **12**, e2020MS002084 (2020).

[16] Vlachas, P. R. *et al.* Backpropagation algorithms and reservoir computing in recurrent neural networks for the forecasting of complex spatiotemporal dynamics. *Neural Networks* **126**, 191–217 (2020).

[17] Maass, W., Natschläger, T. & Markram, H. Real-time computing without stable states: A new framework for neural computation based on perturbations. *Neural computation* **14**, 2531–2560 (2002).

[18] Jaeger, H. & Haas, H. Harnessing nonlinearity: Predicting chaotic systems and saving energy in wireless communication. *Science* **304**, 78–80 (2004).

[19] Karniadakis, G. E. *et al.* Physics-informed machine learning. *Nature Reviews Physics* **3**, 422–440 (2021).

[20] Chen, R. T., Rubanova, Y., Bettencourt, J. & Duvenaud, D. K. Neural ordinary differential equations. *Advances in neural information processing systems* **31** (2018).

[21] Raissi, M., Perdikaris, P. & Karniadakis, G. E. Physics-informed neural networks: A deep learning framework for solving forward and inverse problems involving nonlinear partial differential equations. *Journal of Computational physics* **378**, 686–707 (2019).

[22] Sangiorgio, M. & Dericole, F. Robustness of lstm neural networks for multi-step forecasting of chaotic time series. *Chaos, Solitons & Fractals* **139**, 110045 (2020).

[23] Bhat, U. & Munch, S. B. Recurrent neural networks for partially observed dynamical systems. *Physical Review E* **105**, 044205 (2022).

[24] Yu, R., Zheng, S. & Liu, Y. Learning chaotic dynamics using tensor recurrent neural networks. In *Proceedings of the ICML*, vol. 17 (2017).

[25] Lim, B. & Zohren, S. Time-series forecasting with deep learning: a survey. *Philosophical Transactions of the Royal Society A* **379**, 20200209 (2021).

[26] Tang, Y., Kurths, J., Lin, W., Ott, E. & Kocarev, L. Introduction to focus issue: When machine learning meets complex systems: Networks, chaos, and nonlinear dynamics. *Chaos: An Interdisciplinary Journal of Nonlinear Science* **30**, 063151 (2020).

[27] Godahewa, R., Bergmeir, C., Webb, G. I., Hyndman, R. J. & Montero-Manso, P. Monash time series forecasting archive. *Advances in Neural Information Processing Systems* **1** (2021).

[28] Makridakis, S., Spiliotis, E. & Assimakopoulos, V. M5 accuracy competition: Results, findings, and conclusions. *International Journal of Forecasting* **38**, 1346–1364 (2022).

[29] Costa, A. C., Ahamed, T. & Stephens, G. J. Adaptive, locally linear models of complex dynamics. *Proceedings of the National Academy of Sciences* **116**, 1501–1510 (2019).

[30] Bai, S., Kolter, J. Z. & Koltun, V. An empirical evaluation of generic convolutional and recurrent networks for sequence modeling. *arXiv preprint arXiv:1803.01271* (2018).

[31] Gilpin, W. Chaos as an interpretable benchmark for forecasting and data-driven modelling. *Advances in Neural Information Processing Systems* **1** (2021).

[32] Kantz, H. & Schreiber, T. *Nonlinear time series analysis*, vol. 7 (Cambridge university press, 2004).

[33] Sprott, J. C. Some simple chaotic flows. *Physical review E* **50**, R647 (1994).

[34] Kaptanoglu, A. A., Zhang, L., Nicolaou, Z. G., Fasel, U. & Brunton, S. L. Benchmarking sparse system identification with low-dimensional chaos. *arXiv preprint arXiv:2302.10787* (2023).

[35] Christ, M., Braun, N., Neuffer, J. & Kempa-Liehr, A. W. Time series feature extraction on basis of scalable hypothesis tests (tsfresh—a python package). *Neurocomputing* **307**, 72–77 (2018).

[36] Makowski, D. *et al.* Neurokit2: A python toolbox for neurophysiological signal processing. *Behavior research methods* 1–8 (2021).

[37] McInnes, L., Healy, J., Saul, N. & Großberger, L. Umap: Uniform manifold approximation and projection. *Journal of Open Source Software* **3**, 861 (2018).

[38] Fulcher, B. D., Little, M. A. & Jones, N. S. Highly comparative time-series analysis: the empirical structure of time series and their methods. *Journal of the Royal Society Interface* **10**, 20130048 (2013).

[39] Vlachas, P. R. & Koumoutsakos, P. Learning from predictions: Fusing training and autoregressive inference for long-term spatiotemporal forecasts. *arXiv preprint*

*arXiv:2302.11101* (2023).

[40] Gilpin, W. Recurrences reveal shared causal drivers of complex time series. *arXiv preprint arXiv:2301.13516* (2023).

[41] Herzen, J. *et al.* Darts: User-friendly modern machine learning for time series. *Journal of Machine Learning Research* **23**, 1–6 (2022).

[42] Zeng, A., Chen, M., Zhang, L. & Xu, Q. Are transformers effective for time series forecasting? *arXiv preprint arXiv:2205.13504* (2022).

[43] Zhou, H. *et al.* Informer: Beyond efficient transformer for long sequence time-series forecasting. In *Proceedings of the AAAI conference on artificial intelligence*, vol. 35, 11106–11115 (2021).

[44] Oreshkin, B. N., Carpov, D., Chapados, N. & Bengio, Y. N-BEATS: Neural basis expansion analysis for interpretable time series forecasting. In *International Conference on Learning Representations* (PMLR, 2020).

[45] Challu, C. *et al.* N-HiTS: Neural hierarchical interpolation for time series forecasting. In *Proceedings of the AAAI Conference on Artificial Intelligence* (2023).

[46] Canziani, A., Paszke, A. & Culurciello, E. An analysis of deep neural network models for practical applications. *arXiv preprint arXiv:1605.07678* (2016).

[47] Cvitanović, P. Invariant measurement of strange sets in terms of cycles. *Physical Review Letters* **61**, 2729 (1988).

[48] Kim, J. Z., Lu, Z., Nozari, E., Pappas, G. J. & Bassett, D. S. Teaching recurrent neural networks to infer global temporal structure from local examples. *Nature Machine Intelligence* **3**, 316–323 (2021).

[49] Smith, L. M., Kim, J. Z., Lu, Z. & Bassett, D. S. Learning continuous chaotic attractors with a reservoir computer. *Chaos: An Interdisciplinary Journal of Nonlinear Science* **32**, 011101 (2022).

[50] Sussillo, D. & Abbott, L. F. Generating coherent patterns of activity from chaotic neural networks. *Neuron* **63**, 544–557 (2009).

[51] Martin, C. H., Peng, T. & Mahoney, M. W. Predicting trends in the quality of state-of-the-art neural networks without access to training or testing data. *Nature Communications* **12**, 4122 (2021).

[52] Brown, T. *et al.* Language models are few-shot learners. *Advances in neural information processing systems* **33**, 1877–1901 (2020).

[53] Wolpert, D. H. & Macready, W. G. No free lunch theorems for optimization. *IEEE transactions on evolutionary computation* **1**, 67–82 (1997).